





# Analysis of Periodic Permeability on Free Convective Three-Dimensional Flow with Cattaneo-Christov heat transfer and Slip Effect

Atifa Latif\*, Muhammad Usama Arshad, Muhammad Shoaib

Department of Mathematics, GC University Faisalabad

\*Correspondence: aatifalatif@gmail.com

Citation | Latif. A, Arshad. M. U, Shoaib. M, "Analysis of Periodic Permeability on Free Convective Three-Dimensional Flow with Cattaneo-Christov heat transfer and Slip Effect", IJIST, Vol. 7 Issue. 4 pp 2413-2428, October 2025

Received | Aug 15, 2025 Revised | Sep 09, 2025 Accepted | Sep 11, 2025 Published | October 14, 2025.

The present research paper contributes the slip effects on a three-dimensional viscous fluid flow for free convective boundary conditions with periodic permeability. Free convection fundamentally involves some heat transfer methods. In this work, the Cattaneo-Christov heat transfer method has been employed to develop the knowledge of heat transfer actions in complex flow porous system with periodic permeability. Moreover, the impact of the slip effect is investigated to more effectively deal with the boundary conditions. The mathematical model has designed for incompressible, viscous and laminar flow with free stream specifications. By using the regular perturbation approach, governing highly nonlinear partial differential equations are transferred into the ordinary differential equations in linear form together with certain linear partial differential equations. The separation variables approach is then used for transforming the linear PDEs to ODEs. Analytical solutions are obtained for the pressure, velocity field, components of skin friction, and temperature field. The influence of physical attributes existing in the mathematical representation of the physical occurrence is investigated and illustrated. Both the slip parameter and the Cattaneo-Christov heat flux have an impact of thickness on the thermal boundary layer of observed fluid flow.

Keywords: Cattaneo-Christov Heat Transfer; Free Convective; Periodic Permeability; Slip Effect; Perturbation Method































### **Introduction:**

The occurrence of flows through porous media in nature either for simple fluids or for nanofluids has given high attention in recent years. Numerous scientific and engineering fields have utilized these fluxes, for instance investigations about subterranean supplies for water, riverbed spotting, purifying and filtering techniques in the field of agricultural architecture. The permeable media might have variety of inhomogeneities because it is often not a homogenous channel, in this context, researchers [1][2] examined three-dimensional heat transmission via periodic permeability in a porous material, it might not be required to assume that the porous medium's permeability or suction remain constant. As a result, a sinusoidal permeability of the porous material has been chosen in this research. Vidhya *et al.* [3] have examined convection between two inclined plates that is laminar arranged parallel by supply for warmth and a porous material.

Permeability in free convective fluxes with periodicity appear in variety of engineering and natural phenomena, from geothermal systems to microfluidic devices. The impact of transmission of an incompressible viscous fluid flowing freely convectively when dissipative heat is present has been examined by Manohar *et al.* [4]. Furthermore, the slip effect has been recognized as a critical factor in effectively simulating the boundary conditions in such flows, allowing for a fluid slip at the solid-fluid interface. Makinde [5] examined transmission of mass and heat radiant occur during flow of radiant heat in past traveling through a vertical porosity strip. Singh et al. [6] have conducted a systematic investigation into transverse periodic variation's impact in permeability in relation to heat transfer and free convective flow through a porous medium.

In spite of significance via engineering, particularly aeronautical engineering, laminar flow is a frequently studied field of research that has been the focus of a lot of studies conducted recently. Calculating the drag from frictional objects in a current, such as a plate's drag at zero occurrences or surface drag of an aircraft, is among the most crucial uses of flow that is laminar. Thermal energy is transferred from a hotter to a colder object through heat transfer. Many engineering uses as well as natural phenomena depends on this process. Choudhury et al. [7] analyzed transmission of mass and heat via convection floating viscoelastic motion via periodic permeability in a medium that is porous.

Conductivity, which comes from Fourier's law, continues to be main method of transferring heat in convection. Numerous other fundamental interactions in continuum mechanics, such as the correlation within elasticity or viscous liquids in the tensors of stress and strain, utilize the idea of a straight line between certain quantities. The Christov Cattaneo thermal transmission model for heat in fluid flow is an extension of the law of heat by Fourier's presented by Cattaneo and Christov [8]. Extending the work on heat transfer phenomenon, Nadeem et al. [9] analyzed fluid with stiffness flow using Christov Cattaneo flux mode in the Newtonian fluid presence.

The buoyancy analysis by chemical species and thermal diffusion result in heat transfer. Latif and Rana [10] insight free Convection Jeffery's fluid within Periodic Permeability with the use of the Cattaneo-Christov thermal transfer techniques. Rana and Latif [11] revealed significant finding about free convective flow in three dimensions with periodic permeability of non-Newtonian fluids. The physical aspects of the solid material and fluid of the porous medium are now established to have substantial impact on heat transmission. Han et al. [12] examined the heat transfer and flow in viscoelastic fluid are linked in the heat flow Christov Cattaneo template. The Christov Cattaneo scheme of heat transmission is used to describe thermal transmission in flexible flow affected by an exponentially stretched sheet. There is a narrower hydrodynamic layer at boundary in flexible fluid is thinner. Khan et al. [13] described the flow of three-dimensional and thermal transmission to burg fluid made with Christov Cattaneo thermal flow scheme.



Free convection is a form of heat spread that occurs as a result of changes in fluid density carried on by temperature differences. It emerges when buoyant forces dominate above external forces such as fans or pumps that push the fluid flow like the slippage of fluid. Cao *et al.* [14] investigated the impact of slip on the transmission of heat from vertical plate and mixed convective flow. Vieru et al. [15] discussed the impact of slippage on second-grade fluids' flow of free convection as the exterior temperature rises. Mixed convection occurs when the fluid motion is affected by both buoyant forces and external forces. Javed et al. [16] elaborated the effects of slippage on a third-grade mixed fluid convection flow on an inclined plane near the orthogonal stagnation point. The purpose of the communication of Khan *et al.* [17] is to use the Christov Cattaneo heat flow motion to investigate the stable 3-D boundary layer flow and heat transfer properties to Jeffrey's fluid. The effects of the ratio of stretching rates parameter  $\alpha$  and the thermal relaxation time  $\beta$  on the temperature field are examined and shown graphically. Maxwell fluid flow over 3-D boundary barrier in the plane of a bidirectional stretching surface has examined by Abbasi and Shehzad [18] in relation to the Cattaneo-Christov heat flux model.

Additionally, effects of heat generation or absorption are considered that the fluid's thermal conductivity varies with temperature. A new Christov Cattaneo heat flux template for Jeffrey fluid flow in three dimensions has investigated by Hayat *et al* [19]. A bidirectional extending surface enclosed the flow and the characteristic of thermal relaxation is characterized by warmth transfer using the Cattaneo-Christov heat flux. The results showed that a bigger thermal relaxation parameter has increased a higher heat transfer rate. Shehzad *et al* [20] for 3-D Maxwell liquid, Christov Cattaneo theory of thermal and mass flow towards a moving surface remained the main focus of this study. They created formulations of energy and mass species using the Cattaneo-Christov model of heat and bulk diffusion. The computed results convergent values have visualized using a numerical benchmark. Vasu *et al* [21] using the Cattaneo-Christov heat flux and Buongiorno models, this work examined the free convection flow of Jeffrey nanofluid via a vertical plate with sinusoidal surface temperature and concentration. In contrast to Newtonian nanofluid, Jeffrey nanofluid exhibits a faster velocity but a lower temperature and concentration. Applications for the topic can be found in geothermal systems, petroleum, thermal insulation, and solar collectors.

On various fluidic models, researchers applied Cattaneo-Christov heat transfer technique to discover the new era of heat absorption. Such as, the effects of mass fluxes and Cattaneo-Christov heat on the peristaltic transport of Bingham alumina nanofluid between coaxial vertical tubes have been investigated by El-Dabe *et al* [22]. They observed that with the rise of Bingham parameter there increased the size of trapped bolus and simulating the movements of the stomach fluid during endoscopy. Mabood *et al* [23] elaborated triple diffusion in the natural convection motion of fluid viscosity above horizontal plate in a porous media has in this work. Cattaneo-Christov theories are used to model heat and mass transfer while taking local thermal equilibrium into account.

A three-dimensional mixed convective mass transfer flow over a semi-infinite vertical plate immersed in a porous material has been theoretically studied and described by Ahmed and Choudhury [24]. The novelty of their work has examined how periodic permeability affects flow and transport properties when viscous dissipation and chemical reactions are present. Gupta *et al.* [25] investigated the solutions with different intensities of magnetic fields Jeffrey nano liquid Darcy–Forchheimmer flow across a permeable cone using Christov Cattaneo bulk and heat flux theories. The impact of Christov Cattaneo mass and warmth flow techniques on transmission of warmth and mass in single-phase Jeffrey nanofluid flow across a porous sphere has examined by them.

The goal of current study is to investigate 3-dimensional free convection flow via Periodically exposed extremely porous media to permeability and its implications on the



Cattaneo- Christov method of thermal transfer rate. The fascinating dynamics of the convective transfer of heat process are introduced by the phenomena of slip when fluid particles adjacent to the solid surface encounter reduced friction. Three-dimensional fluid flows are essential to study because most real-world motions are intrinsically three-dimensional. Few main objectives can be discussed for studying 3D slip effect of periodic permeable fluid flow through porous medium such as realistic flow behavior around aircraft wings, in blood vessels or in turbines can be captured with accurate description of velocity, pressure, and temperature fields. Cross flow effects which normally negligible in 2D flows but 3D models clearly identify the effects of cross flow as well as vortices and swirl motions.

# Mathematical Representation:

Suppose that a highly porous and permeable material encircled by an infinitely permeable plate is being used to study whether a viscous, incompressible fluid behaves as it passes through it. The x-axis is associated with the plates of vertical surface, and the plate is vertically oriented in the x-z plane. The y-axis is designated as being in line with the plane of plate, parallel to its surface, and pointing in the guidance of the consistent free streaming velocity U. Suppose that the permeable medium displays periodicity (Figure  $1^{\otimes}$ ), which has the following form. Consider

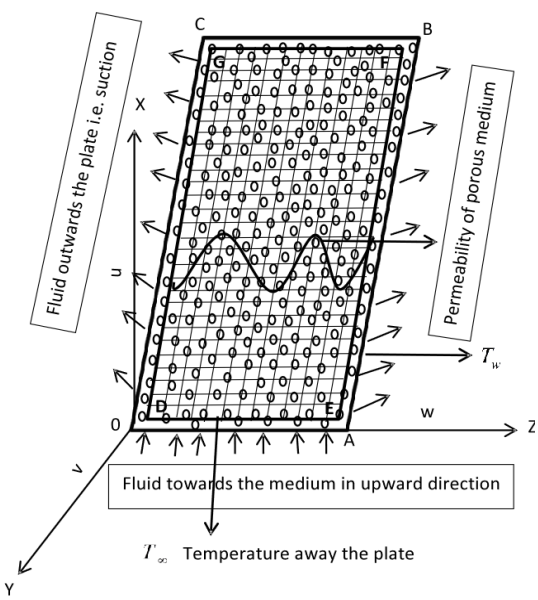


**Figure 1.** Geometry of Flow

$$K^{\otimes}(z^{\otimes}) = \frac{K_0^{\otimes}}{(1 + \varepsilon \cos \pi z^{\otimes} / l)}, \tag{1}$$

is the presence of periodic permeability variation in the medium of pores, permeability variation's wavelength l, and ( $\varepsilon$  <<1) is its amplitude. The change in permeability introduces the possibility of a three-dimensional nature to the problem. In the body force term, just the impact of the density  $\rho$  fluctuation with temperature distribution T is evaluated, and all flow rates are believed to be constant.

# Modeling in Mathematics:

We have the equation for energy, continuity and momentum for viscous incompressible fluid as:

$$\nabla . \vec{V} = 0, \tag{2}$$

$$\rho \frac{d\vec{V}}{dt} = \nabla \cdot \tau, \tag{3}$$



$$\rho \frac{d\zeta}{dt} = -\nabla . \overrightarrow{q}, \tag{4}$$

Where  $\zeta = c_p T = -k\nabla T$ , T is the temperature,  $c_p$  is the specific heat at constant pressure  $\nabla$  is the vector operator, k is the thermal conductivity,  $\rho$  is the density of the fluid, and  $\tilde{\tau}$  is the Cauchy stress tensor.

The velocity component suggested by, the following procedure control the flow via highly porous material.  $u^{\otimes}, v^{\otimes}, w^{\otimes}$  in the  $x^{\otimes}, z^{\otimes}, y^{\otimes}$ -directions, respectively.  $u^{\otimes}, w^{\otimes}, v^{\otimes}, K^{\otimes}$ ,  $T_w^{\otimes}, p^{\otimes}$  and  $T_w^{\otimes}$  are all in the form of dimensional parameters. Where the symbol " $_{\otimes}$ " is used for dimensional values.

$$\frac{\partial v^{\otimes}}{\partial v^{\otimes}} + \frac{\partial w^{\otimes}}{\partial z^{\otimes}} = 0, \tag{5}$$

$$v^{\otimes} \frac{\partial u^{\otimes}}{\partial y^{\otimes}} + w^{\otimes} \frac{\partial u^{\otimes}}{\partial z^{\otimes}} = g \beta (T^{\otimes} - T_{\infty}^{\otimes}) + \upsilon \left( \frac{\partial^{2} u^{\otimes}}{\partial y^{\otimes 2}} + \frac{\partial^{2} u^{\otimes}}{\partial z^{\otimes 2}} \right) - \frac{\upsilon}{K^{\otimes}} (u^{\otimes} - U), \quad (6)$$

$$v^{\otimes} \frac{\partial v^{\otimes}}{\partial y^{\otimes}} + w^{\otimes} \frac{\partial v^{\otimes}}{\partial z^{\otimes}} = -\frac{1}{\rho} \frac{\partial p^{\otimes}}{\partial y^{\otimes}} + \upsilon \left( \frac{\partial^{2} v^{\otimes}}{\partial y^{\otimes 2}} + \frac{\partial^{2} v^{\otimes}}{\partial z^{\otimes 2}} \right) - \frac{\upsilon}{K^{\otimes}} v^{\otimes}, \tag{7}$$

$$v^{\otimes} \frac{\partial w^{\otimes}}{\partial y^{\otimes}} + w^{\otimes} \frac{\partial w^{\otimes}}{\partial z^{\otimes}} = -\frac{1}{\rho} \frac{\partial p^{\otimes}}{\partial z^{\otimes}} + \upsilon \left( \frac{\partial^{2} w^{\otimes}}{\partial y^{\otimes 2}} + \frac{\partial^{2} w^{\otimes}}{\partial z^{\otimes 2}} \right) - \frac{\upsilon}{K^{\otimes}} w^{\otimes}, \tag{8}$$

$$v^{\otimes} \frac{\partial T^{\otimes}}{\partial y^{\otimes}} + w^{\otimes} \frac{\partial T^{\otimes}}{\partial z^{\otimes}} = \frac{k}{\rho c_{p}} \left( \frac{\partial^{2} T^{\otimes}}{\partial y^{\otimes 2}} + \frac{\partial^{2} T^{\otimes}}{\partial z^{\otimes 2}} \right)$$

$$-\lambda \left[ v^{\otimes 2} \frac{\partial^2 T^{\otimes}}{\partial y^{\otimes 2}} + w^{\otimes 2} \frac{\partial^2 T^{\otimes}}{\partial z^{\otimes 2}} + 2v^{\otimes} w^{\otimes} \frac{\partial^2 T^{\otimes}}{\partial y^{\otimes} \partial z^{\otimes}} + \right.$$

$$\left(v^{\otimes} \frac{\partial v^{\otimes}}{\partial y^{\otimes}} + w^{\otimes} \frac{\partial v^{\otimes}}{\partial z^{\otimes}}\right) \frac{\partial T^{\otimes}}{\partial y^{\otimes}} + \left(v^{\otimes} \frac{\partial w^{\otimes}}{\partial y^{\otimes}} + w^{\otimes} \frac{\partial w^{\otimes}}{\partial z^{\otimes}}\right) \frac{\partial T^{\otimes}}{\partial z^{\otimes}}\right],\tag{9}$$

The variables that follow are the problem's boundary conditions:

$$At \ y^{\otimes} = 0; \ v^{\otimes} = -V, \ u^{\otimes} = \gamma^{\otimes} \frac{\partial u^{\otimes}}{\partial y^{\otimes}}, \ w^{\otimes} = 0, \ T^{\otimes} = T_{w}^{\otimes},$$

$$At \ y^{\otimes} \to \infty; \ w^{\otimes} = 0, \ u^{\otimes} = U, \ p^{\otimes} = p_{\infty}^{\otimes}, \ T^{\otimes} = T_{\infty}^{\otimes}.$$

$$(10)$$

where  $T_w^{\otimes}$  and  $T_\infty^{\otimes}$  are the temperature distant from the plane and the plate's temperature at fixed pressure  $p_\infty^{\otimes}$  in the free stream. g be the fluid flow's force of gravity in the x-axis, and V>0 is the fixed vacuum velocity and adverse indication typically from the plates suction.

The non-dimensional variables defined below are given.

$$y = \frac{y^{\otimes}}{l}, z = \frac{z^{\otimes}}{l}, u = \frac{u^{\otimes}}{U}, v = \frac{v^{\otimes}}{V},$$

$$w = \frac{w^{\otimes}}{V}, p = \frac{p^{\otimes}}{\rho V^{2}}, \theta = \frac{T^{\otimes} - T_{\infty}^{\otimes}}{T_{w}^{\otimes} - T_{\infty}^{\otimes}},$$
(11)

The equations (5) to (9) consequently have the following form:



$$\frac{\partial v}{\partial v} + \frac{\partial w}{\partial z} = 0 \tag{12}$$

$$v\frac{\partial u}{\partial y} + w\frac{\partial u}{\partial z} = G\operatorname{Re} + \frac{1}{\operatorname{Re}} \left( \frac{\partial^2 u}{\partial y^2} + \frac{\partial^2 u}{\partial z^2} \right) - \frac{(u-1)(1+\cos\pi z)}{\operatorname{Re}K_0}$$
(13)

$$v\frac{\partial v}{\partial y} + w\frac{\partial v}{\partial z} = -\frac{\partial p}{\partial y} + \frac{1}{\text{Re}} \left( \frac{\partial^2 u}{\partial y^2} + \frac{\partial^2 u}{\partial z^2} \right) - \frac{(1 + \varepsilon \cos \pi z)v}{\text{Re} K_0}$$
 (14)

$$v\frac{\partial v}{\partial y} + w\frac{\partial v}{\partial z} = -\frac{\partial p}{\partial z} + \frac{1}{\text{Re}} \left( \frac{\partial^2 u}{\partial y^2} + \frac{\partial^2 u}{\partial z^2} \right) - \frac{(1 + \varepsilon \cos \pi z)w}{\text{Re} K_0}$$
 (15)

$$v\frac{\partial\theta}{\partial y} + w\frac{\partial\theta}{\partial z} = \frac{1}{\operatorname{Re}\operatorname{Pr}} \left( \frac{\partial^2\theta}{\partial y^2} + \frac{\partial^2\theta}{\partial z^2} \right)$$

$$-L\left[v^2\frac{\partial^2\theta}{\partial y^2} + w^2\frac{\partial^2\theta}{\partial z^2} + 2vw\frac{\partial^2\theta}{\partial y\partial z}\right]$$

$$+\left(v\frac{\partial v}{\partial y}+w\frac{\partial v}{\partial z}\right)\frac{\partial \theta}{\partial y}+\left(v\frac{\partial w}{\partial y}+w\frac{\partial w}{\partial z}\right)\frac{\partial \theta}{\partial z}$$
(16)

The designing boundary conditions vary:

$$At y = 0; v = -1, u = \gamma \frac{\partial u}{\partial y}, w = 0, \theta = 1,$$

$$At y \to \infty; w = 0, u = 1, p = p_{\infty}, \theta = 0.$$

$$(17)$$

Even the Prandtl, Grashof, and elastic parameters, as well as the permeability and Reynolds numbers, are all assigned as below:

$$\Pr = \frac{\mu c_p}{k}, \text{Prandtl number, } G = \frac{\upsilon g \beta \left(T_w^{\otimes} - T_\infty^{\otimes}\right)}{UV^2}, \text{Grashof number,}$$

$$L = \frac{V\lambda}{l}$$
, Elastic parameter,  $K_0 = \frac{K_0^{\otimes}}{l^2}$ , Permeability parameter,

$$Re = \frac{Vl}{v}$$
, Reynolds number

### The Mathematical Formulation for Solution:

We assume preceding for solution of equations in the locale of the medium (12) - (16):

$$d = d_0 + \varepsilon d_1 + \varepsilon^2 d_2 + \dots$$
 (18)

Where  $\varepsilon$  is a microscopic factor and d represents any of v, w, p, u and  $\theta$ .

## Model in Two-Dimensions:

When  $\varepsilon = 0$ , the three-dimensional problem's complexity decreases by reducing it to a two-dimensional analysis flow of free convection within a permeable medium. The system's behaviors are controlled by the following equations:

$$\frac{dv_0}{dy} = 0 ag{19}$$

$$\frac{d^2 u_0}{dy^2} - v_0 \operatorname{Re} \frac{du_0}{dy} - \frac{u_0}{K_0} = -G \operatorname{Re}^2 \theta - \frac{1}{K_0}, \tag{20}$$



$$\frac{d^2 v_0}{dy^2} - v_0 \operatorname{Re} \frac{dv_0}{dy} - \frac{v_0}{K_0} = \operatorname{Re} \frac{dp_0}{dy},$$
 (21)

$$\frac{d^2 w_0}{dv^2} - v_0 \operatorname{Re} \frac{dw_0}{dv} - \frac{w_0}{K_0} = 0$$
 (22)

$$(1 - v_0^2 \text{Re Pr}) \frac{d^2 \theta}{dy^2} - v_0 \text{Re Pr} \frac{d\theta_0}{dy} = 0$$
 (23)

The suitable boundary conditions vary:

$$At \ y = 0; \ u_0 = \gamma \frac{\partial u_0}{\partial y}, \ v_0 = -1, \quad \theta_0 = 1,$$

$$At \ y \to \infty; \ u_0 = 1, \ p = p_{\infty}, \ \theta_0 = 0$$
(24)

We obtain the solution to the two-dimensional problem after significant calculation:

$$u_0 = \left(\frac{\gamma MG\lambda_0 + G\lambda_0 - 1}{1 + \gamma\lambda}\right) e^{-\lambda y} + 1 - G\lambda_0 e^{-My} , \qquad (25)$$

$$v_0 = -1, w_0 = 0 \text{ and } p_0 = p_\infty,$$
 (26)

$$\theta_0 = e^{-My}, \tag{27}$$

Here, 
$$M = \frac{\text{Re Pr}}{1 - L \text{Re Pr}}$$
 but  $1 - L \text{Re Pr} < 1$ 

Were,

$$\lambda_0 = \frac{\text{Re}^2}{\frac{\text{Re}^2 \, \text{Pr}}{1 - L \, \text{Re} \, \text{Pr}} (\frac{\text{Pr}}{1 - L \, \text{Re} \, \text{Pr}} - 1) - \frac{1}{K_0}} \text{ and } \lambda = \frac{\text{Re}}{2} + \sqrt{\frac{\text{Re}^2}{4} + \frac{1}{K_0}}.$$

### **Three-Dimensional Model:**

When  $\varepsilon \neq 0$  the resulting equations are a set of initial order differential equations.

$$\frac{\partial v_1}{\partial y} + \frac{\partial w_1}{\partial z} = 0 \tag{28}$$

$$v_1 \frac{\partial u_0}{\partial y} - \frac{\partial u_1}{\partial y} = G \operatorname{Re} \theta_1 + \frac{1}{\operatorname{Re}} \left( \frac{\partial^2 u_1}{\partial y^2} + \frac{\partial^2 u_1}{\partial z^2} \right) - \frac{1}{\operatorname{Re} K_0} \left\{ (u_0 - 1) \cos \pi z + u_1 \right\}$$
 (29)

$$-\frac{\partial v_1}{\partial y} = -\frac{\partial p_1}{\partial y} + \frac{1}{\text{Re}} \left( \frac{\partial^2 v_1}{\partial y^2} + \frac{\partial^2 v_1}{\partial z^2} \right) - \frac{1}{\text{Re} K_0} (v_1 - \cos \pi z)$$
 (30)

$$-\frac{\partial w_1}{\partial y} = -\frac{\partial p_1}{\partial z} + \frac{1}{\text{Re}} \left( \frac{\partial^2 w_1}{\partial y^2} + \frac{\partial^2 w_1}{\partial z^2} \right) - \frac{w_1}{\text{Re} K_0}$$
(31)

$$v_{1} \frac{\partial \theta_{0}}{\partial y} - \frac{\partial \theta_{1}}{\partial y} = \frac{1}{\text{Re Pr}} \left( \frac{\partial^{2} \theta_{1}}{\partial y^{2}} + \frac{\partial^{2} \theta_{1}}{\partial z^{2}} \right) - L \left[ \frac{\partial^{2} \theta_{1}}{\partial y^{2}} - 2v_{1} \frac{d^{2} \theta_{0}}{dy^{2}} - \frac{\partial v_{1}}{\partial y} \frac{d\theta_{0}}{dy} \right]$$
(32)

The suitable conditions at the boundary are as follows

$$At \ y = 0; \ u_1 = \gamma \frac{\partial u_1}{\partial y}, \ v_1 = 0, \ w_1 = 0, \ \theta_1 = 0$$

$$At \ y \to \infty; \ u_1 = 0, \ w_1 = 0, \ p_1 = 0, \ \theta_1 = 0$$
(33)

The Flow Field Solution:



PDEs that clarify 3-D flow of free convection are expressed via equations (29) to (33). We presume  $v_1$ ,  $w_1$  and  $p_1$  of the form that follows:

$$v_{1}(y,z) = -v_{11}(y)\cos \pi z,$$

$$w_{1}(y,z) = \frac{1}{\pi}v'_{11}(y)\sin \pi z,$$

$$p_{1}(y,z) = p_{11}(y)\cos \pi z$$
(34)

The design for  $w_1(x, y)$  and  $v_1(x, y)$  has been chosen to guarantee that the equation for continuity (28) is satisfied. Putting equation (34) into equations (30) and (31), we get

$$v_{11}'' + \operatorname{Re}v_{11}' - (\pi^2 + \frac{1}{K_0})v_{11} = -\operatorname{Re}p_{11}' + \frac{1}{K_0},$$
(35)

$$v_{11}''' + \operatorname{Re} v_{11}'' - (\pi^2 + \frac{1}{K_0})v_{11}' = -\pi^2 \operatorname{Re} p_{11}.$$
 (36)

To get rid of the pressure  $p_{11}$ , equations (35) and (36) have to be resolved simultaneously to yield the differential equation given as follows:

$$v_{11}^{i\nu} + \operatorname{Re}v_{11}^{\prime\prime\prime} - (2\pi^2 + \frac{1}{K_0})v_{11}^{\prime\prime} - \pi^2 \operatorname{Re}v_1^{\prime} + (\pi^4 + \frac{\pi^2}{K_0})v_{11} = -\frac{\pi^2}{K_0}.$$
 (37)

Solve equation (37) under the convection conditions to get  $v_1$  and  $w_1$ , we have

$$v_1(y,z) = \frac{1}{(\pi - \lambda_1)(\pi^2 K_0 + 1)} (\pi e^{-\lambda_1 y} - \lambda e^{-\pi y} - \pi + \lambda_1) \cos \pi z, \tag{38}$$

$$w_1(y,z) = \frac{\lambda_1}{(\pi - \lambda_1)(\pi^2 K_0 + 1)} (e^{-\pi y} - e^{-\lambda_1 y}) \sin \pi z.$$
 (39)

# Temperature & Pressure Profiles:

Equations (35) and (36) can be solved concurrently with the updated conditions at the boundary (33), the pressure value can be obtained as follows:

$$p_{1}(y,z) = \frac{\lambda_{1} \left(\pi \operatorname{Re} + \frac{1}{K_{0}}\right)}{\pi \operatorname{Re}(\pi - \lambda_{1})(\pi^{2}K_{0} + 1)} e^{-\pi y} \cos \pi z.$$
(40)

To find an expression, we employ the temperature distribution.

$$\theta_1(y,z) = \theta_{11}(y)\cos \pi z. \tag{41}$$

Subject to the following boundary conditions,

$$\theta_{11}(0) = 0$$
,  $\theta_{11}(\infty) = 0$ ,

yields

$$\theta_{1}(y,z) = \left\{ \frac{M \operatorname{Re} \operatorname{Pr}}{(\pi - \lambda_{1})(\pi^{2} K_{0} + 1)} \left[ 2LM \left( A e^{-(\lambda_{1} + M)y} - A_{11} e^{-(\pi + M)y} + (A_{12} - A_{13}) e^{-My} \right) \right. \\ \left. + \pi \lambda_{1} L \left( A_{14} e^{-(\lambda_{1} + M)y} - A_{15} e^{-(\pi + M)y} \right) + \left( A e^{-(\lambda_{1} + M)y} - A_{11} e^{-(\pi + M)y} + (A_{12} - A_{13}) e^{-My} \right) \right] \\ \left. - \frac{M \operatorname{Re} \operatorname{Pr}}{(\pi - \lambda_{1})(\pi^{2} K_{0} + 1)} \left[ 2LM \left( A - A_{11} + A_{12} - A_{13} \right) + \pi \lambda_{1} L \left( A_{14} + A_{15} \right) + A - A_{11} + A_{12} - A_{13} \right] e^{-\beta y} \right\} \cos \pi z.$$

Wherever

$$\lambda_1 = \frac{\text{Re}}{2} + \sqrt{\frac{\text{Re}}{4} + (\pi^2 + \frac{1}{K_0})}$$



#### Main Flow:

To attain result of velocity of primary motion, we presume that

$$u_1(y,z) = u_{11}(y)\cos \pi z.$$
 (43)

We may answer this for  $u_1$  by putting the expressions (43) into (29) under the following equivalent improved conditions at boundary

$$u_{11}(0) = 0, \ u_{11}(\infty) = 0,$$

yields

$$\begin{split} u_{1}(y,z) &= \left[ \frac{MG \operatorname{Re}^{3} \operatorname{Pr}}{(\pi - \lambda_{1})(\pi^{2} K_{0} + 1)(1 + y\lambda_{1})} \{ [2LM(A_{16} - A_{17} + C_{11}) + \pi \lambda_{1}(C_{12} - C_{13}) + A_{16} - A_{17} + C_{11}] \right. \\ &- \left[ (2LM(A - A_{11} + A_{12} - A_{13}) + \pi \lambda_{1} L(A_{14} - A_{15}) + (A - A_{11} + A_{12} - A_{13})]C_{4} \right\} \\ &- \frac{\operatorname{Re}}{(1 + y\lambda)(\pi - \lambda_{1})(\pi^{2} K_{0} + 1)(1 + y\lambda_{1})} \left[ B_{22} - \frac{(1 + y\lambda)}{(\pi^{2} + \frac{1}{K_{0}})} \right] \\ &+ \frac{1}{(1 + y\lambda)} (B_{23}) - \frac{yG \operatorname{Re}^{3} \operatorname{Pr} M}{(\pi - \lambda_{1})(\pi^{2} K_{0} + 1)} \{ [2LM(-(\lambda_{1} + M)A_{16} + (\pi + M)A_{17} - MC_{11})] - (2LM(A - A_{11} + A_{12} - A_{13}) - \pi \lambda_{1} L(A_{14} - A_{15}) + (-(\lambda_{1} + M)A_{16} + (\pi + M)A_{17} - MC_{11})] - (2LM(A - A_{11} + A_{12} - A_{13}) - \pi \lambda_{1} L(A_{14} - A_{15}) \\ &+ A - A_{11} + A_{12} - A_{13} - \beta C_{14} \right\} - \frac{y \operatorname{Re}}{(1 + y\lambda)(\pi - \lambda_{1})(\pi^{2} K_{0} + 1)(1 + y\lambda_{1})} \\ &- (\pi + \lambda)B_{15} + (\pi + \lambda)B_{16} + MB_{17} - \frac{(1 + y\lambda)}{(\pi^{2} + \frac{1}{K_{0}})} + \\ &- \frac{y}{(1 + y\lambda)(1 + y\lambda_{1})} \left[ -\lambda B_{18} - \lambda B_{19} + \lambda B_{20} + MB_{21} \right] e^{-\lambda y} \\ &- \frac{yG \operatorname{Re}^{3} \operatorname{Pr} M}{(\pi - \lambda_{1})(\pi^{2} K_{0} + 1)} \{ [2LM(A_{16} e^{-(\lambda + M)y} - A_{17} e^{-(\pi + M)} + C_{11} e^{-My}) + \\ \pi \lambda_{1}L(C_{12} e^{-(\lambda_{1} + M)y} - C_{13} e^{-(\pi + M)y}) + A_{16} e^{-(\lambda + M)y} - A_{17} e^{-(\pi + M)} + C_{11} e^{-My} \} \\ &- \frac{\operatorname{Re}}{(1 + y\lambda)(\pi - \lambda_{1})(\pi^{2} K_{0} + 1)} \left[ -B_{11} e^{-(\lambda_{1} + \lambda)y} - B_{12} e^{-(\lambda_{1} + \lambda)y} + B_{13} e^{-(\lambda_{1} + \lambda)y} \\ &+ B_{14} e^{-(\pi + \lambda)y} + B_{15} e^{-(\pi + \lambda)y} - B_{10} e^{-(\pi + \lambda)y} - B_{12} e^{-(\lambda_{1} + \lambda)y} - A_{17} e^{-(\lambda_{1} + \lambda)y} \\ &+ \frac{1}{1 + y2} (B_{18} e^{-\lambda y} + B_{19} e^{-(x + \lambda)}) - B_{10} e^{-(x + \lambda)y} - B_{17} e^{-My} \right] \cos \pi \pi z. \end{split}$$

Where,

$$\beta = \frac{H}{2} + \sqrt{\frac{H^2}{4} + \frac{\pi^2}{1 - L \operatorname{Re} \operatorname{Pr}}}$$

The fixed involved in the solution of equations (42) & (44) are below here:

$$A = \frac{\pi}{(\lambda_{1} + A_{1})^{2} - A_{1}(\lambda_{1} + A_{1}) - \frac{\pi^{2}}{1 - L \operatorname{Re} \operatorname{Pr}}}, A_{11} = \frac{\lambda_{1}}{(\pi + A_{1})^{2} - A_{1}(\pi + A_{1}) - \frac{\pi^{2}}{1 - L \operatorname{Re} \operatorname{Pr}}}$$

$$A_{12} = \frac{1 - L \operatorname{Re} \operatorname{Pr}}{\pi}, A_{13} = \frac{\lambda_{1}(1 - L \operatorname{Re} \operatorname{Pr})}{\pi^{2}}, A_{14} = \frac{1}{(\lambda_{1} + A_{1})^{2} - A_{1}(\lambda_{1} + A_{1}) - \frac{\pi^{2}}{1 - L \operatorname{Re} \operatorname{Pr}}}$$



$$A_{15} = \frac{1}{(\pi + H)^2 - H(\pi + H) - \frac{\pi^2}{1 - L \operatorname{Re} \operatorname{Pr}}}, \quad A_{16} = \frac{A}{(\lambda_1 + H)^2 - \operatorname{Re}(\lambda_1 + H) - (\pi^2 + \frac{1}{K_0})}$$

$$A_{17} = \frac{A_{11}}{(\pi + M)^2 - \operatorname{Re}(\pi + M) - (\pi^2 + \frac{1}{K_0})}, \quad C_{11} = \frac{A_{12} - A_{13}}{M^2 - \operatorname{Re}M - (\pi^2 + \frac{1}{K_0})}$$

$$C_{12} = \frac{A_{14}}{(\lambda_1 + M)^2 - \operatorname{Re}(\lambda_1 + M) - (\pi^2 + \frac{1}{K_0})}, \quad C_{13} = \frac{A_{15}}{(\pi + M)^2 - \operatorname{Re}(\pi + M) - (\pi^2 + \frac{1}{K_0})}$$

$$C_{14} = \frac{1}{\beta^2 - \operatorname{Re}\beta - (\pi^2 + \frac{1}{K_0})}, \quad B_{11} = \frac{\gamma G \lambda_0 M \pi \lambda_1}{(\lambda_1 + \lambda)^2 - \operatorname{Re}(\lambda_1 + \lambda) - (\pi^2 + \frac{1}{K_0})}$$

$$B_{12} = \frac{\pi \lambda_1 G \lambda_0}{(\lambda_1 + \lambda)^2 - \operatorname{Re}(\lambda_1 + \lambda) - (\pi^2 + \frac{1}{K_0})}, \quad B_{13} = \frac{\pi \lambda_1}{(\lambda_1 + \lambda)^2 - \operatorname{Re}(\lambda_1 + \lambda) - (\pi^2 + \frac{1}{K_0})}$$

$$B_{14} = \frac{\gamma \pi \lambda_1 M G \lambda_0}{(\pi + \lambda)^2 - \operatorname{Re}(\pi + \lambda) - (\pi^2 + \frac{1}{K_0})}, \quad B_{15} = \frac{G \lambda_1 \lambda_0 \pi}{(\pi + \lambda)^2 - \operatorname{Re}(\pi + \lambda) - (\pi^2 + \frac{1}{K_0})}$$

$$B_{16} = \frac{\pi \lambda_1}{(\pi + \lambda)^2 - \operatorname{Re}(\pi + \lambda) - (\pi^2 + \frac{1}{K_0})}, \quad B_{17} = \frac{(1 + \gamma \lambda) G \lambda_0}{H^2 - \operatorname{Re}H - (\pi^2 + \frac{1}{K_0})},$$

$$B_{18} = \frac{\gamma M G \lambda_0}{K_0 [\lambda^2 - \operatorname{Re}\lambda - (\pi^2 + \frac{1}{K_0})]}, \quad B_{19} = \frac{G \lambda_0}{K_0 [\lambda^2 - \operatorname{Re}\lambda - (\pi^2 + \frac{1}{K_0})]}$$

$$B_{20} = \frac{1}{K_0 [\lambda^2 - \operatorname{Re}\lambda - (\pi^2 + \frac{1}{K_0})]}, \quad B_{21} = \frac{(1 + \gamma \lambda) G \lambda_0}{K_0 [H^2 - \operatorname{Re}H - (\pi^2 + \frac{1}{K_0})]}$$

$$B_{22} = -B_{11} - B_{12} + B_{13} + B_{14} + B_{15} - B_{16} - B_{17}$$

$$B_{23} = B_{18} + B_{19} + B_{13} - B_{20}$$

### **Skin Friction:**

Deriving essential specific parameters like the component of skin friction becomes attainable once the velocity profile is obtained. The non-dimensional skin friction component in the *x*-direction can be expressed as fellow:

$$\tau_x^{\otimes} = \frac{\tau_{yx}}{\rho UV} = \frac{\upsilon}{Vl} \left( \frac{\partial u}{\partial y} \right)_{v=0}$$
 (45)

Eliminating the sign of "\otimes" for convenience, we have result:

$$\tau_x = H_0 + \varepsilon H_1 \cos \pi z. \tag{46}$$

Where

$$H_0 = \frac{1}{\text{Re}} \left( \frac{du_0}{dy} \right)_{y=0} \& H_1 = \frac{1}{\text{Re}} \left( \frac{du_{11}}{dy} \right)_{y=0}$$



### **Heat Flow:**

The Nusselt number, which indicates the rate of heat transmission, can be determined by comparing transfer of heat factor of the temperature field.

$$N = \frac{-q}{\rho V c_p (T_W^{-1} - T_\infty^{-1})}.$$
(47)

While we nondimensional and ease the result equation (48), we get

$$N = \frac{k}{\rho V c_p l} \left( \frac{\partial \theta}{\partial y} \right)_{y=0} = \frac{1}{\text{Re Pr}} \left( \frac{d\theta_0}{dy} + \varepsilon \frac{d\theta_{11}}{dy} \cos \pi z \right)_{y=0}$$
$$= S_0 + \varepsilon S_1 \cos \pi z. \tag{48}$$

### Results and Discussion:

This research model aimed to investigate the theoretical aspects of the Christov Cattaneo heat transfer method involving slip effects in the context of 3-D flows of free convection occurring in a periodic permeable medium that is porous. Analytical solutions occured for the pressure, temperature distribution, velocity field and components of skin friction. Graphical illustrations showed the impact of dimensionless parameters on various parameters including Grashof number (G), Reynolds number (Re), Prandtl number (Pr), Permeability parameter  $K_0$ , and elastic parameter (L).

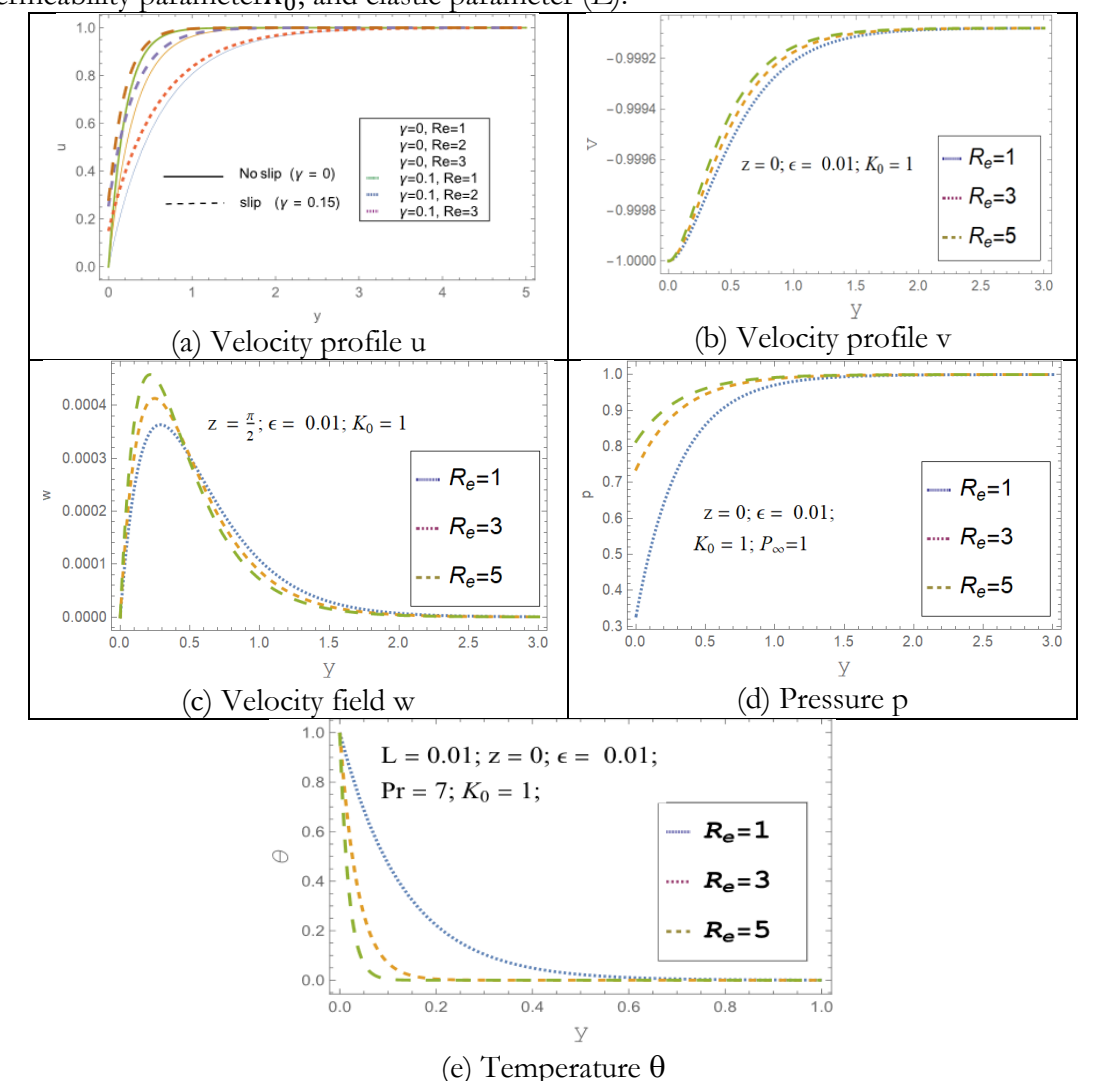


Figure 2. Velocity, pressure and temperature fields are impacted by Reynolds number

If the values of all other nondimensional parameters remained the same and ( $\varepsilon = 0.01$ , Pr=7,  $K_0=1$ , L=0.01, G=1,  $\chi=0$ ,  $\gamma=1$ ) with slip conditions and the Reynolds number varies: Re = 1, 3, 5. Figure 1 illustrated the influence of Reynolds number on temperature distribution, pressure and velocity field. When the Reynolds number rises, that is seen that the primary flow velocity component, u Figure 1(a), increases. Furthermore, the Figure 1(a) showed both effects that is with slip and without slip and clearly the presence of a slip parameter velocity significantly improves the primary flow velocity. From a mathematical point of view, it is definitely appropriate to claim that the presence of slip at the plate in the direction of primary motion results to a decrease in adhesive forces. Therefore, the decreasing behaviour resulted in an expansion of the velocity component in the direction of the main flow. The point of most significant velocity is observed at the free layer. Moreover, the inclusion of a slip parameter reasons a decrease in the thickness of the boundary layer. The Reynolds number rises as the dimension of velocity field  $\nu$  Figure 1(b) rises. However, it is mentioned that as we travel away from the plate, the amplitude of this velocity component reduces, which seems to be a physically reasonable result. The velocity component w Figure 1(c) increased rapidly as it approached the plate, reaches its highest value, then rapidly decreases until it ultimately converges to zero as  $y \to \infty$ . It should be observed that this velocity component increased as Re, the Reynolds number, increases. Physically, this suggests that gravitational forces have become more beneficial than viscous forces nearby to the plate. In Figure 1(d), the pressure increased in addition to rise in the Reynolds number Re adjacent to the plate. At the free surface it becomes more valuable. The Reynolds number Re affected the temperature distribution is shown in Figure 1(e). It demonstrates that the temperature boundary surface falls as Re increased.

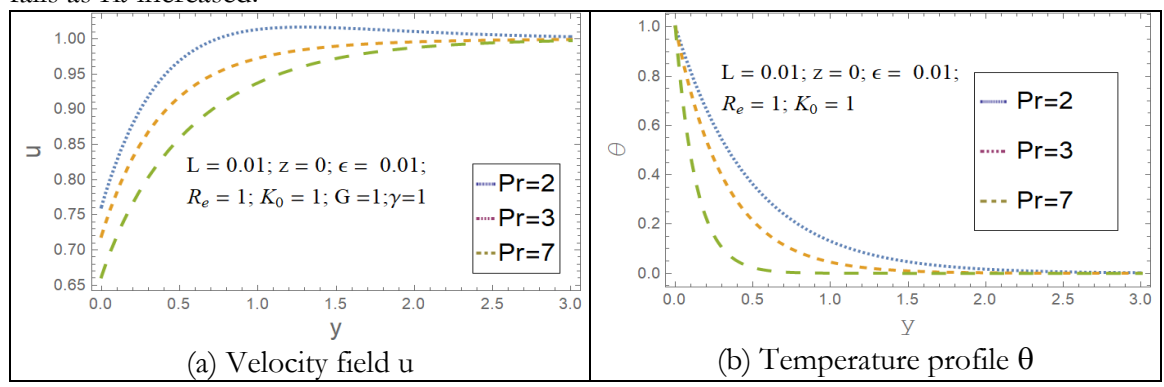


Figure 3. Temperature and velocity field is influenced by Prandtl numbers

Figure 2 illustrated the way the temperature field and the main flow u affected by the Prandtl number. Figure 2(a) demonstrates that the slip parameter and the Prandtl number have an impact on the main velocity profile u. The results of this study show that falls in the velocity component is correlated with a rise in the Prandtl number. The graphic represented in Figure 2(b) has readily apparent that when the Prandtl number Pr increases, the temperature of the fluid falls. Figure 2(b) causing thermal boundary layer to become thinner. The fluid's low thermal conductivity at high Prandtl numbers caused a drop in the thermal layer's thickness. The result consequently provided persuasive proof for the physical principle that the Prandtl number increases as the boundary layer thickness reduces.

In Figure 3, the Permeable parameter is varied:  $K_0$ =0.1, 0.5, 1. whenever any beyond no dimensional parameters under fixed ( $\varepsilon$ =0.01,  $\chi$ =0, Pr=7,  $K_0$ =1, L=0.01, G=1). Figure 3(a) showed how permeable parameter  $K_0$  impact on velocity profile u. It can be seen that the primary flow velocity begins to falls as  $K_0$  rises. The slip parameter remained to exert an important effect on the increase of component of velocity. According to Figure 3(b), the permeability parameter  $K_0$  has a comparable impact on the velocity profile v. The velocity



profile w, according to Figure 3(c) increased exponentially adjacent to plate, obtains its extreme value, decreases swiftly, and eventually converges to zero as  $y \to \infty$ . This is valid for a fixed value of  $K_0$ . As the permeable parameter  $K_0$  near plate increased, the pressure rises Figure 4(d). The influence of permeable parameter  $K_0$  on the field of temperature is perceived in Figure 3(e). It has been perceived that the permeable parameter  $K_0$  and the temperature

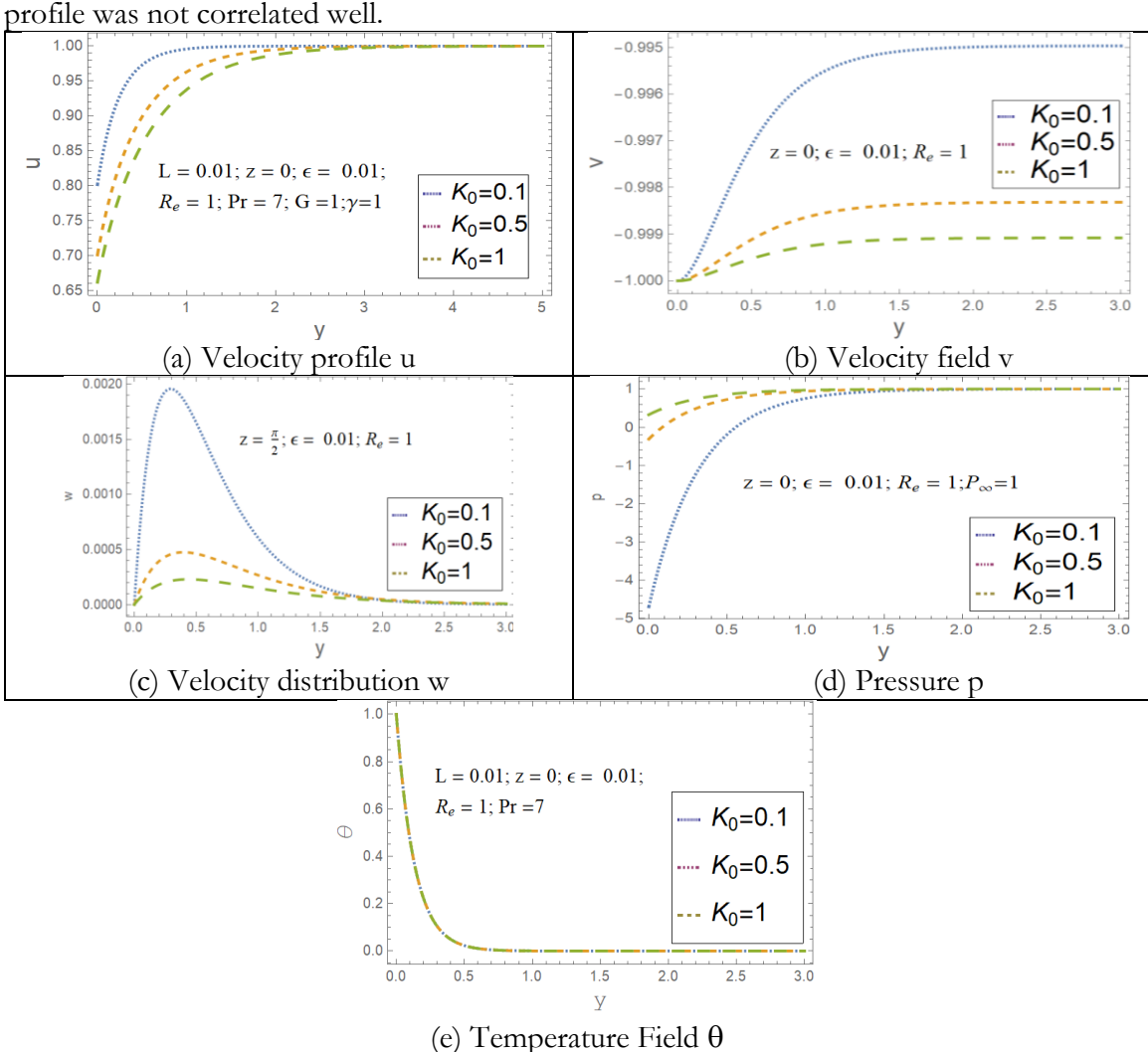
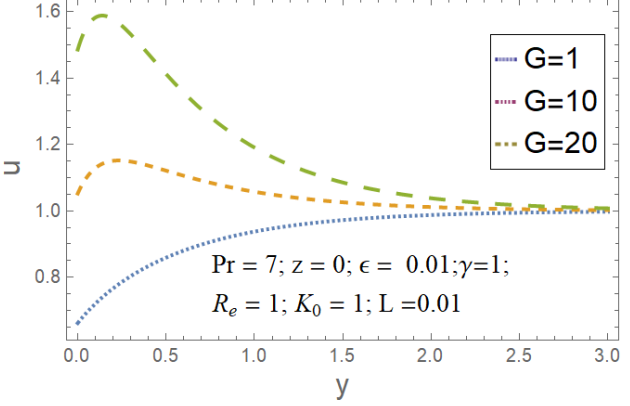


Figure 4. Velocity, pressure and temperature fields affected by Permeability parameter



**Figure 5.** The main flow is impacted by Grashof number



Figure 4 displayed the Grashof number and how it affects the main velocity u for plate conditioning. The impact of the free convection parameter, namely the Grashof number, on the primary motion velocity field u due to planes low temperature.

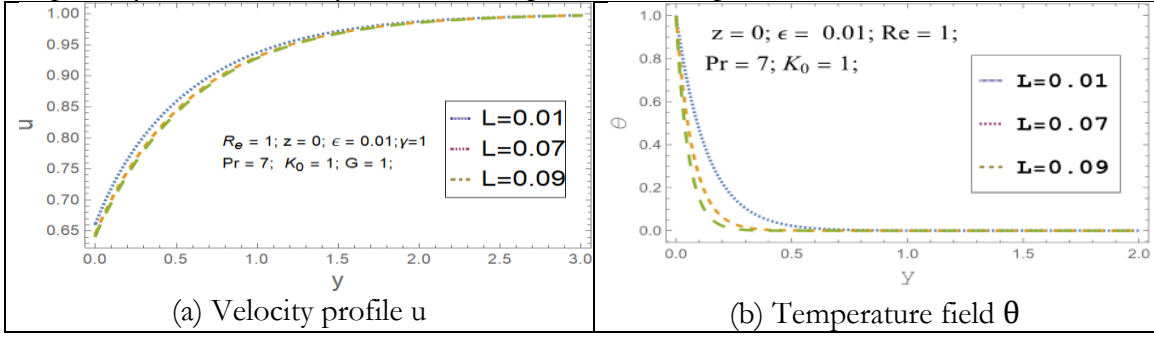


Figure 6. The main flow and temperature field are impacted by Elastic parameter

In Figure 5, the Elastic parameter varied: L=0.01, 0.07, and 0.09. Whenever any additional dimensionless limitations remained constant ( $\varepsilon$ =0.01,  $\chi$ =0, Pr=7,  $K_0$ =1,  $R_0$ =1,  $R_0$ =1,  $R_0$ =1). The main flow  $R_0$  Figure 5(a) are affected by the Elastic parameter. The presented graph in Figure 5(a) illustrated a negative correlation between the Elastic parameter and the velocity component, indicating that an increase in the former results in a decrease in the other. The graphical representation clearly demonstrated that an increase in the Elastic parameter  $R_0$  Consequently, this leads to a decrease in the level of the fluid field, as shown in Figure 5(b). Consequently, this leads to a decrease in the level of the thermal boundary layer. The low thermal conductivity of the fluid at high elastic parameters resulted in a decrease in the thickness of the thermal layer.

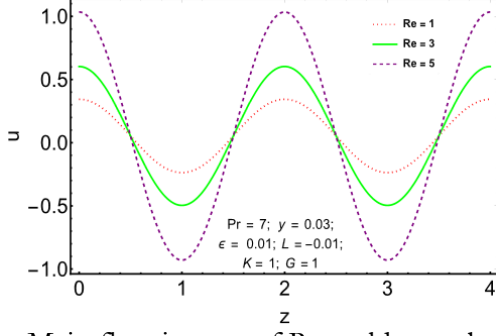


Figure 7. The Main flow impact of Reynolds number along z-axis

Figure 6 demonstrated the influence of Reynolds number on main flow velocity profile along z-axis. Figure 6 depicted the horizontal view of main flow velocity where the normal value was flat and it was appropriate to claim that the presence of slip at the plate in the direction of primary motion resulted to a decrease in adhesive forces.

Here in this study, it is observed that a strong correlation exists the current and earlier results described [6][11] which supports the correctness of the computational approach.

# **Conclusion:**

A detailed description of Christov Cattaneo heat transfer method with slip effect through porous medium with periodic permeability is presented analytically. Through a comprehensive analysis, the main observation can be drawn:

The Cattaneo-Christov thermal transfer model, that includes non-local heat conduction into consideration, exerted an important effect on the fluid's temperature distribution.

Compared to the classic Fourier's law, the Cattaneo-Christov model introduced a delay to the fluid's thermal response. As a result, there was a change in the time it required for the fluid to attain its steady-state temperature.



Slip conditions at the solid-fluid contact exerted an effect on the fluid velocity distribution, modifying the boundary layer's viscosity and the flow properties.

Both the slip conditions and Christov Cattaneo heat transmission method have an impact on depth of thermodynamics boundary layers. The combined impact of these effects changed how quickly heat flowed from the solid surface into the fluid, and exerted an impact on the convective heat transfer process as an entire.

The Cattaneo-Christov model and slip effect may improve or suppress heat transport, depending on the particular conditions and variables.

### **References:**

- [1] K. D. Singh, K. Chand, and G. N. Verma, "Heal Transfer in a Three-Dimensional Flow through a Porous Medium with Periodic Permeability," *ZAMM J. Appl. Math. Mech. / Zeitschrift für Angew. Math. und Mech.*, vol. 75, no. 11, pp. 950–952, Jan. 1995, doi: 10.1002/zamm.19950751112;journal:journal:15214001;wgroup:string:publication.
- [2] A. Raptis, C. Perdikis, and G. Tzivanidis, "Free convection flow through a porous medium bounded by a vertical surface," *J. Phys. D. Appl. Phys.*, vol. 14, no. 7, p. L99, Jul. 1981, doi: 10.1088/0022-3727/14/7/001.
- [3] S. Vidhya, M., & Kesavan, "Laminar convection through porous medium between two vertical parallel plates with heat source," *Front. Automob. Mech. Eng.*, pp. 197–200, 2010.
- [4] V. M. Soundalgekar, R. M. Lahurikar, and S. G. Pohanerkar, "Transient free convection flow of an incompressible viscous dissipative fluid," *Heat Mass Transf. und Stoffuebertragung*, vol. 32, no. 4, pp. 301–305, 1997, doi: 10.1007/S002310050125/METRICS.
- [5] O. D. Makinde, "Free convection flow with thermal radiation and mass transfer past a moving vertical porous plate," *Int. Commun. Heat Mass Transf.*, vol. 32, no. 10, pp. 1411–1419, 2005, doi: https://doi.org/10.1016/j.icheatmasstransfer.2005.07.005.
- [6] R. S. K. D. Singh, "Three-dimensional free convective flow and heat transfer through a porous medium with periodic permeability," *Indian J. Pure Appl. Math.*, vol. 33, no. 6, 2002, [Online]. Available: https://www.researchgate.net/publication/266016303\_Three-dimensional\_free\_convective\_flow\_and\_heat\_transfer\_through\_a\_porous\_medium\_with\_periodic\_permeability
- [7] D. D. Rita Choudhury, "Free convective visco-elastic flow with heat and mass transfer through a porous medium with periodic permeability," *Int. J. Heat Mass Transf.*, vol. 53, no. 9–10, pp. 1666–1672, 2010, doi: https://doi.org/10.1016/j.ijheatmasstransfer.2010.01.023.
- [8] C. I. Christov, "On frame indifferent formulation of the Maxwell–Cattaneo model of finite-speed heat conduction," *Mech. Res. Commun.*, vol. 36, no. 4, pp. 481–486, 2009, doi: https://doi.org/10.1016/j.mechrescom.2008.11.003.
- [9] S. A. Sohail Nadeem and Noor Muhammad, "Cattaneo-Christov flux in the flow of a viscoelastic fluid in the presence of Newtonian heating," *J. Mol. Liq.*, vol. 237, pp. 180–184, 2017, doi: https://doi.org/10.1016/j.molliq.2017.04.080.
- [10] M. A. R. Atifa Latif, "Analysis of Free Convective Jeffery's Fluid with Periodic Permeability and Cattaneo-Christov Heat Transfer," *IFAC-PapersOnLine*, vol. 51, pp. 155–160, 2018, doi: https://doi.org/10.1016/j.ifacol.2018.11.278.
- [11] A. Latif, M. A. Rana, and M. Hussan, "Periodic permeable free convective 3-dimensional flow of a second grade fluid with slip effect," *Phys. Scr.*, vol. 96, no. 8, p. 085207, May 2021, doi: 10.1088/1402-4896/ABC282.
- [12] X. Z. Shihao Han, Liancun Zheng, Chunrui Li, "Coupled flow and heat transfer in viscoelastic fluid with Cattaneo–Christov heat flux model," *Appl. Math. Lett.*, vol. 38, pp. 87–93, 2014, doi: https://doi.org/10.1016/j.aml.2014.07.013.
- [13] W. A. K. Masood Khan, "Three-dimensional flow and heat transfer to burgers fluid using Cattaneo-Christov heat flux model," *J. Mol. Liq.*, vol. 221, pp. 651–657, 2016, doi: https://doi.org/10.1016/j.molliq.2016.06.041.



- [14] K. Cao and John Baker, "Slip effects on mixed convective flow and heat transfer from a vertical plate," *Int. J. Heat Mass Transf.*, vol. 52, no. 15–16, pp. 3829–3841, 2009, doi: https://doi.org/10.1016/j.ijheatmasstransfer.2009.02.013.
- [15] D. Vieru, M. A. Imran, and A. Rauf, "Slip effect on free convection flow of second grade fluids with ramped wall temperature," *Heat Transf. Res.*, vol. 46, no. 8, pp. 713–724, 2015, doi: 10.1615/HEATTRANSRES.2015007464.
- [16] T. Javed and I. Mustafa, "Slip effects on a mixed convection flow of a third-grade fluid near the orthogonal stagnation point on a vertical surface," *J. Appl. Mech. Tech. Phys.*, vol. 57, no. 3, pp. 527–536, May 2016, doi: 10.1134/S0021894416030172/METRICS.
- [17] M. I. Khan, T. Hayat, M. Waqas, A. Alsaedi, and M. I. Khan, "Effectiveness of radiative heat flux in MHD flow of Jeffrey-nanofluid subject to Brownian and thermophoresis diffusions," *J. Hydrodyn.*, vol. 31, no. 2, pp. 421–427, Apr. 2019, doi: 10.1007/S42241-019-0003-7/METRICS.
- [18] S. A. Abbasi, F. M., & Shehzad, "Heat transfer analysis for three-dimensional flow of Maxwell fluid with temperature dependent thermal conductivity: application of Cattaneo-Christov heat flux model," *J. Mol. Liq.*, vol. 220, pp. 848–854, 2016.
- [19] A. A. Tasawar Hayat, Taseer Muhammad, Meraj Mustafa, "Three-dimensional flow of Jeffrey fluid with Cattaneo-Christov heat flux: An application to non-Fourier heat flux theory," *Chinese J. Phys.*, vol. 55, no. 3, pp. 1067–1077, 2017, doi: https://doi.org/10.1016/j.cjph.2017.03.014.
- [20] S. A. Shehzad, T. Hayat, A. Alsaedi, and M. A. Meraj, "Cattaneo-Christov heat and mass flux model for 3D hydrodynamic flow of chemically reactive Maxwell liquid," *Appl. Math. Mech. (English Ed.*, vol. 38, no. 10, pp. 1347–1356, Oct. 2017, doi: 10.1007/S10483-017-2250-6/METRICS.
- [21] B. Vasu, A. K. Ray, and R. S. R. Gorla, "Free convective heat transfer in Jeffrey fluid with suspended nanoparticles and Cattaneo–Christov heat flux," *Proc. Inst. Mech. Eng. Part N J. Nanomater. Nanoeng. Nanosyst.*, vol. 234, no. 3–4, pp. 99–114, Jul. 2020, doi: 10.1177/2397791420912628;wgroup:string:publication.
- [22] N. T. M. El-Dabe, M. Y. Abou-Zeid, M. E. Oauf, D. R. Mostapha, and Y. M. Mohamed, "Cattaneo–Christov heat flux effect on MHD peristaltic transport of Bingham Al2O3 nanofluid through a non-Darcy porous medium," *Int. J. Appl. Electromagn. Mech.*, vol. 68, no. 1, pp. 59–84, 2022, doi: 10.3233/JAE-210057.
- [23] F. Mabood, T. A. Yusuf, S. A. Shehzad, and I. A. Badruddin, "Cattaneo–Christov model for triple diffusive natural convection flows over horizontal plate with entropy analysis embedded in porous regime," *Proc. Inst. Mech. Eng. Part C J. Mech. Eng. Sci.*, vol. 236, no. 9, pp. 4776–4790, May 2022, doi: 10.1177/09544062211057831;PAGE:STRING:ARTICLE/CHAPTER.
- [24] N. Ahmed and K. Choudhury, "Heat and mass transfer in three-dimensional flow through a porous medium with periodic permeability," *Heat Transf. Asian Res.*, vol. 48, no. 2, pp. 644–662, Mar. 2019, doi: 10.1002/HTJ.21399;JOURNAL:JOURNAL:15206556;requestedjournal:journal:15231496;wgroup:string:publication.
- [25] S. Gupta, S. Gupta, and A. Sharma, "Darcy–Forchheimmer flow of MHD Jeffrey nanoliquid over a permeable cone with Cattaneo–Christov heat and mass flux theories," *Indian J. Phys.*, vol. 96, no. 2, pp. 503–513, Feb. 2022, doi: 10.1007/S12648-020-01985-Z/METRICS.



Copyright © by authors and 50Sea. This work is licensed under Creative Commons Attribution 4.0 International License.